Article

Nerve-independent formation of a topologically complex postsynaptic apparatus

Terrance T. Kummer, Thomas Misgeld, Jeff W. Lichtman, and Joshua R. Sanes

Department of Anatomy and Neurobiology, Washington University School of Medicine, St. Louis, MO 63110

As the mammalian neuromuscular junction matures, its acetylcholine receptor (AChR)–rich postsynaptic apparatus is transformed from an oval plaque into a pretzel-shaped array of branches that precisely mirrors the branching pattern of the motor nerve terminal. Although the nerve has been believed to direct postsynaptic maturation, we report here that myotubes cultured aneurally on matrix-coated substrates form elaborately branched AChR-rich domains remarkably similar to those seen in vivo. These domains share several characteristics with the mature postsynaptic apparatus, including colocalization of multiple postsynaptic markers, clustering of subjacent myonuclei, and dependence on the muscle-specific kinase and rapsyn for their formation. Time-lapse imaging showed that branched structures arise from plaques by formation and fusion of AChR-poor perforations through a series of steps mirroring that seen in vivo. Multiple fluorophore imaging showed that growth occurs by circumferential, asymmetric addition of AChRs. Analysis in vivo revealed similar patterns of AChR addition during normal development. These results reveal the sequence of steps by which a topologically complex domain forms on a cell and suggest an unexpected nerve-independent role for the postsynaptic cell in generating this topological complexity.

Introduction

Synaptic development occurs in a series of steps through which pre- and postsynaptic structures are assembled, mature, and become precisely apposed to each other. These processes have been particularly well studied at the skeletal neuromuscular junction (NMJ; for review see Sanes and Lichtman, 1999). At the rodent NMJ, for example, the acetylcholine receptor (AChR)–rich postsynaptic apparatus is initially small and plaque shaped, and then develops multiple regions of lower AChR density during the first two postnatal weeks. These areas enlarge and elaborate in parallel with their motor innervation, ultimately forming precisely matched, pretzel-like arrays of pre- and postsynaptic branches (Steinbach, 1981; Slater, 1982a; Marques et al., 2000). At the same time, the molecular architecture of the maturing synapse becomes more complex (for reviews see Patton, 2000; Sanes and Lichtman, 2001). A central question in the analysis of these processes is which are cell-autonomous and which require interactions between pre- and postsynaptic elements.

It has long been known that myotubes cultured in the absence of neurons form small, specialized domains, some-times called "hot spots" or "plaques," in which AChRs cluster at high density (Vogel et al., 1972; Fischbach and Cohen, 1973; Anderson and Cohen, 1977; Bloch, 1979). This result, coupled with recent genetic studies in vivo, led to the idea that muscle cells can initiate postsynaptic differentiation independent of the nerve (Sanes and Lichtman, 2001; Arber et al., 2002). In contrast, the topologically complex pretzel-like arrays typical of the mature synapse have never been observed to form in the absence of innervation either in vitro or in vivo. Additionally, neurites contacting myotubes in vitro can induce AChR clusters with shapes mirroring those of the neurite–myotube contact (Anderson and Cohen, 1977; Frank and Fischbach, 1979), and neonatal denervation in vivo arrests the morphological maturation of AChR aggregates (Slater 1982b; Moss and Schuetze, 1987). Based on these observations, it is generally assumed that the branching pattern of the motor axon dictates the topology of the mature postsynaptic apparatus.

Here, we present data that call this assumption into question. While studying AChR clustering in aneural, cultured myotubes, we found conditions that promoted formation of complex, branched receptor aggregates resembling those found at adult NMJs. Further analysis revealed many parallels

Address correspondence to Joshua R. Sanes, Dept. of Anatomy and Neurobiology, Washington University School of Medicine, 660 South Euclid Ave., St. Louis, MO 63110. Tel.: (314) 362-2507. Fax: (314) 747-1150. email: sanesj@pcg.wustl.edu

Key words: acetylcholine receptor; laminin; muscle; neuromuscular junction; synapse formation
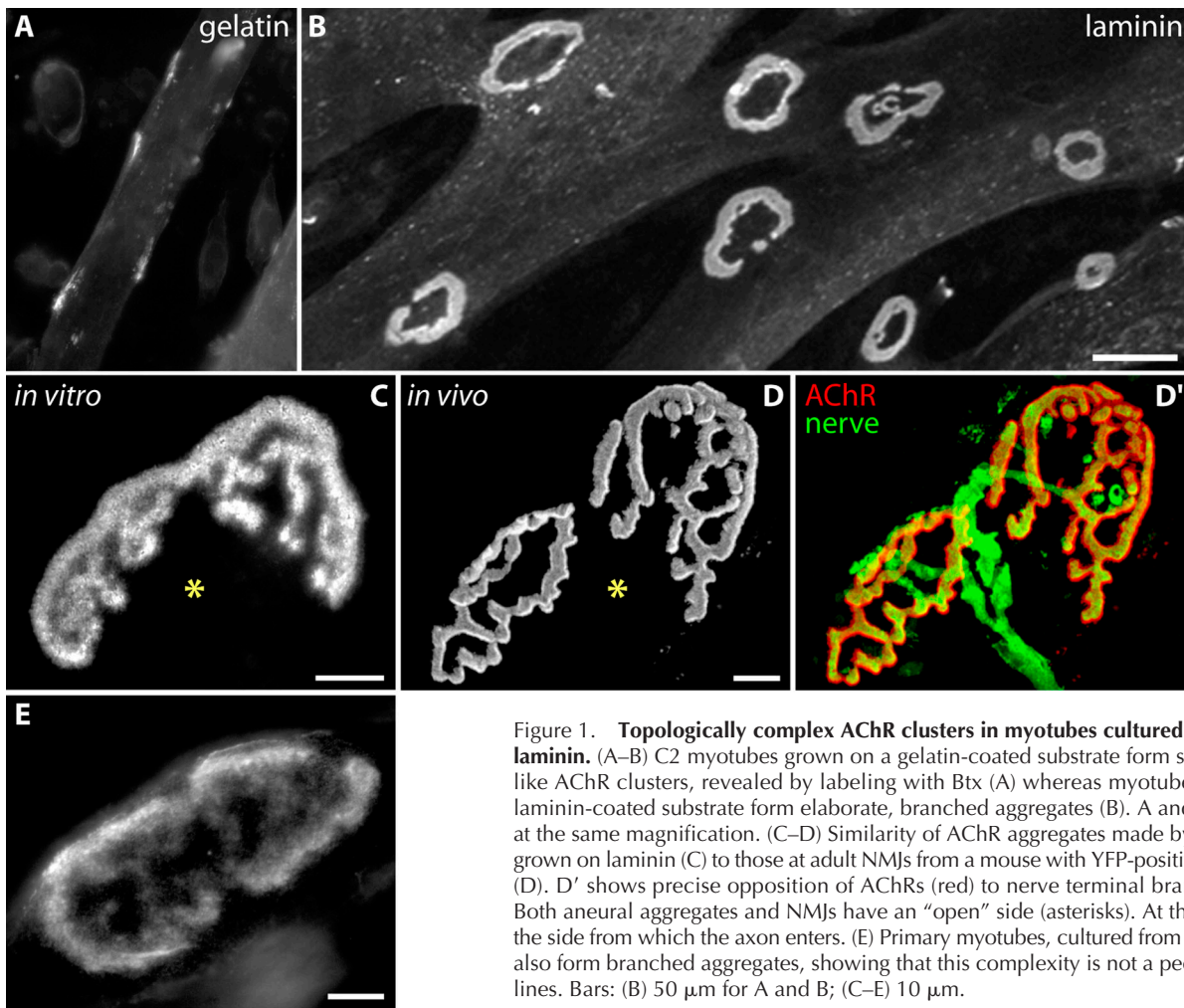
Figure 1. **Topologically complex AChR clusters in myotubes cultured aneurally on laminin.** (A–B) C2 myotubes grown on a gelatin-coated substrate form simple plaque-like AChR clusters, revealed by labeling with Btx (A) whereas myotubes grown on a laminin-coated substrate form elaborate, branched aggregates (B). A and B are shown at the same magnification. (C–D) Similarity of AChR aggregates made by C2 myotubes grown on laminin (C) to those at adult NMJs from a mouse with YFP-positive motor axons (D). D′ shows precise opposition of AChRs (red) to nerve terminal branches (green). Both aneural aggregates and NMJs have an "open" side (asterisks). At the NMJ, this is the side from which the axon enters. (E) Primary myotubes, cultured from neonatal mice, also form branched aggregates, showing that this complexity is not a peculiarity of cell lines. Bars: (B) 50 μm for A and B; (C–E) 10 μm.

between these aggregates and the adult postsynaptic apparatus, including association with a similar set of molecular specializations, dependence on rapsyn and the muscle-specific kinase (MuSK) for their formation, and maturation through a similar series of transitional forms. We then exploited the experimental accessibility of the preparation to document the steps and patterns of AChR addition and removal that transform the plaque into a pretzel. Finally, we performed experiments in vivo to show that patterns of AChR addition discovered in vitro actually occur during synaptogenesis. Together, these results reveal nerve-independent mechanisms that can specify many features of the mature postsynaptic apparatus, and raise the possibility that the muscle plays an instructive role in shaping the nerve terminal arbor as the synapse matures.

Results

Formation of complex AChR clusters in the absence of innervation

Cells of the C2 mouse myogenic line grow as myoblasts in serum-rich medium, and then fuse to form myotubes after transfer to serum-poor medium (Yaffe and Saxel, 1977). Even in the absence of neurons, myogenesis is accompanied by up-regulation of many genes involved in formation of the postsynaptic apparatus, including those encoding AChR subunits. When myotubes are grown on gelatin-coated substrates, some of the AChRs form high density hot spots that can be labeled with the specific ligand, α-bungarotoxin (Btx; Fig. 1 A). Hot spots are generally <20 μm in the longest dimension and lack complex internal structure, resembling in these respects the AChR clusters that form initially in vivo (Sanes and Lichtman, 2001).

While studying AChR clustering in C2 cells, we discovered that myotubes grown for several days on substrates coated with the matrix molecule laminin assembled AChR aggregates that were larger and geometrically more complex than those reported previously (Fig. 1, B and C; see Fig. 5 J for quantitation). These AChR-rich domains formed exclusively at the substrate–myotube interface. Complex aggregates also formed in primary myotubes (Fig. 1 E) and in other cells lines cultured under similar conditions (Fig. 2, A–F), showing that they are not a peculiarity of the C2 line or of cell lines in general. Importantly, we never observed such complex aggregates on myotubes cultured on gelatin, even those matched for age or diameter.

Complex receptor clusters on C2 cells shared the following features with NMJs. First, they were composed of branches arrayed in a pretzel-shaped pattern closely resembling that observed at innervated junctions in vivo (Fig. 1, C and D).
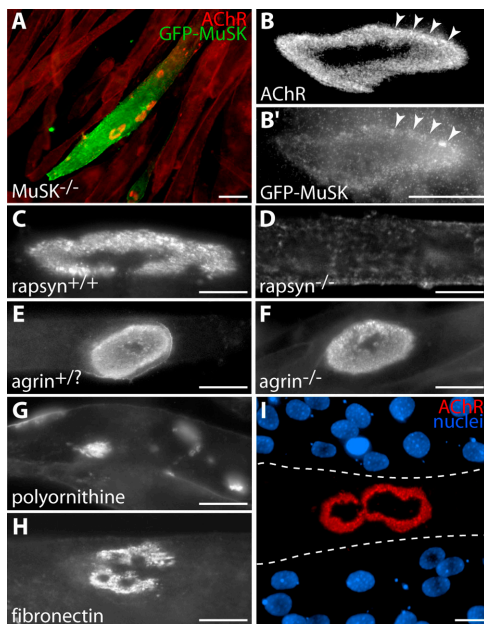
Figure 2. **Requirements for formation of branched AChR aggregates on laminin-coated substrates.** (A–B) MuSK is required. Myotubes from a MuSK$^{-/-}$ cell line form no AChR aggregates when cultured on laminin-coated substrates. AChRs are instead distributed uniformly over their surface (cells stained uniformly red with Btx). When transfected with GFP-MuSK (green), such cells form receptor aggregates (red) with complex morphology (A). High power view shows colocalization of these aggregates (B) with GFP-MuSK (B'). Arrowheads mark corresponding points in B and B'. (C and D) Rapsyn is required. Myotubes from a control cell line form complex AChR aggregates when cultured on laminin (C), but myotubes from a rapsyn$^{-/-}$ cell line form no clusters (D). (E and F) Agrin is not required. Primary myotubes from controls (E, agrin$^{+/?}$, meaning heterozygous or wild type) and agrin$^{-/-}$ (F) mice both form complex clusters on laminin-coated substrates. (G) Polyornithine-coated substrates do not support complex AChR aggregate formation in C2 cells. AChR aggregates in these cultures are plaque shaped. (H) Laminin is not required. C2 myotubes form branched aggregates on fibronectin-coated substrates, although they are generally smaller and less complex than those that develop on laminin-coated substrates. (I) When C2 myotubes are mechanically detached from laminin-coated substrata, postsynaptic "ghosts" labeled with Btx (red) remain attached to the substrate. Nuclear staining with DAPI (blue) shows that there is no myotube over the receptor aggregate. Dotted lines indicate approximate borders of the former myotube. Bars: (A) 100 μm; (B'–I) 20 μm.

Second, their size (23–94 μm along their long axis; mean = 46 μm for aggregates with at least one branch; $n = 102$), was similar to that observed for adult mouse NMJs. Third, complex aneural clusters, like NMJs, were generally oblong, with a long axis parallel to that of the myotube and one end larger than the other. Finally, aneural AChR clusters, like NMJs, were frequently "open" on one side (Fig. 1, C and D, asterisk). Interestingly, in vivo, the nerve enters the synapse at the open side (Fig. 1, D and D'), but our results show that nerves are not necessary for aggregates to become polarized.

## MuSK- and rapsyn-dependent formation of aneural aggregates

Clustering of AChRs at the NMJ requires MuSK; no AChR clusters form in muscles of MuSK$^{-/-}$ or rapsyn$^{-/-}$ mice (DeChiara et al., 1996; Sanes and Lichtman, 2001). On the

other hand, some agents, including soluble laminin, can stimulate MuSK-independent clustering of AChRs in cultured myotubes (Sugiyama et al., 1997; Gautam et al., 1999). At least in this respect, soluble laminin clusters AChRs by a mechanism of unknown physiological significance. To ask whether laminin-coated substrata promoted formation of aggregates by the physiologically relevant MuSK-dependent mechanism, we used a myogenic cell line derived from MuSK$^{-/-}$ mice. These muscle cells form small AChR clusters when treated with soluble laminin (Sugiyama et al., 1997), but did not form AChR clusters when cultured on laminin-coated substrates (Fig. 2 A, red cells). Transfection of the cells with GFP-tagged MuSK, however, restored their ability to form complex AChR aggregates (Fig. 2, A and B, green cell). Thus, unlike bath-applied laminin but like the mechanisms responsible for receptor clustering at the NMJ, substrate-bound laminin requires MuSK to form aneural AChR aggregates. We also tested myotubes from rapsyn$^{-/-}$ mice, because rapsyn, like MuSK, is required for all AChR clustering in vivo. Rapsyn$^{-/-}$ myotubes cultured on laminin-coated substrates formed no receptor clusters, although control cells did (Fig. 2, C and D).

AChR clusters are dramatically perturbed in mice lacking agrin, which activates MuSK (Gautam et al., 1996; Burgess et al., 1999). Agrin is expressed by myotubes as well as by motorneurons, but only the latter synthesize the alternatively spliced z-plus agrin isoform which is ~1,000-fold more effective than z-minus agrin in promoting AChR clustering (Ferns et al., 1992; Gesemann et al., 1995). Nonetheless, z-minus agrin does have detectable clustering activity in some assays (Ferns et al., 1992). Therefore, we considered the possibility that matrix-coated substrates might act by concentrating muscle-derived z-minus agrin, or even by inducing expression of z-plus agrin. To test this hypothesis, we assayed primary myotubes cultured from mice lacking all forms of agrin (Lin et al., 2001). When such cells were grown on laminin-coated substrates, AChR clusters formed that were identical to those observed on myotubes prepared from control littermates (Fig. 2, E and F). This result is consistent with the finding that MuSK can be activated in the absence of agrin (Zhou et al., 1999; Lin et al., 2001). Likewise, adding soluble agrin to myotubes cultured on gelatin increased the number of plaques but never led to formation of more complex aggregates (unpublished data).

We also asked if formation of aneural pretzels was a specific response to laminin. Neither gelatin nor polyornithine induced aneural pretzel formation (Fig. 1 A and Fig. 2 G). However, branched structures were observed when myotubes were cultured on a substrate coated with fibronectin (Fig. 2 H). These clusters were smaller than those formed on laminin, and had more jagged edges, but their presence demonstrated that the ability to induce branched aggregates is not unique to laminin. Instead, it may be that strong adhesion promotes topological maturation (see Discussion). Consistent with this possibility, myotubes adhered more strongly to laminin or fibronectin than to gelatin or polyornithine (as determined by susceptibility to mechanical detachment; not depicted), and myotubes detached from laminin-coated substrates left behind patterned AChR aggregates, presumably embedded in adherent membrane fragments (Fig. 2 I).

AChR   antigen
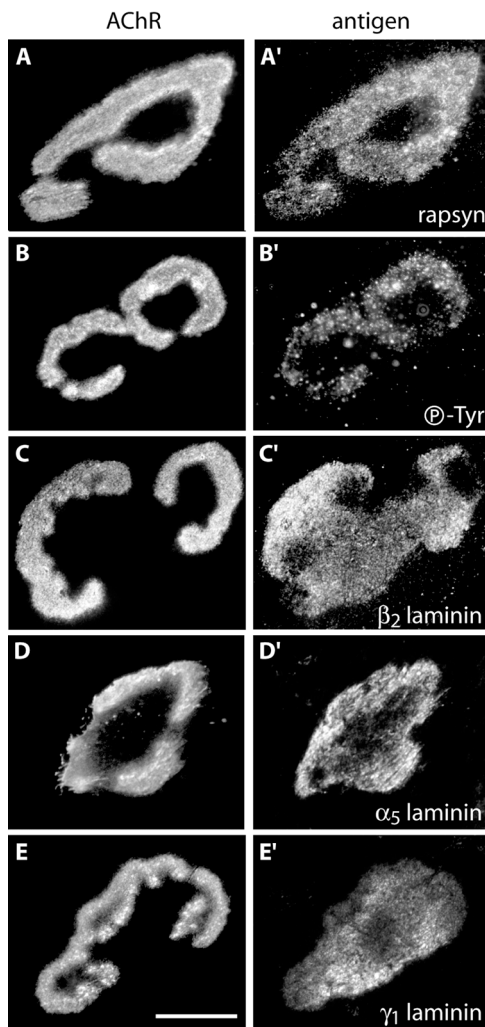
Figure 3.   **Colocalization of AChRs and other postsynaptic markers in aneural myotubes cultured on laminin.** Myotubes were double stained with Btx (A–E) and antibodies to rapsyn (A'), phosphotyrosine (B'), laminin β2 (C'), laminin α5 (D'), or laminin γ1 (E'). Bar, 20 μm for all panels.

Molecular features shared by aneural aggregates and NMJs

To compare the molecular architecture of aneural aggregates and NMJs, we used a panel of probes to matrix, membrane, and cytoplasmic proteins known to be concentrated at synaptic sites in vivo (Sanes and Lichtman, 1999, 2001). The distribution of rapsyn, as revealed by immunostaining, precisely matched that of AChRs in aggregates, as it does in vivo (Fig. 3 A; Sanes and Lichtman, 1999, 2001). Similarly, MuSK was enriched in AChR-rich areas, as monitored by the localization of GFP-MuSK in transfected myotubes (Fig. 2 B), although some GFP-MuSK was present in AChR-poor areas, perhaps as a consequence of overexpression. Likewise, phosphotyrosine staining was increased at areas rich in AChRs (Fig. 3 B; Qu et al., 1990). Thus, signaling components involved in NMJ differentiation are associated with aneural aggregates.

The association of synaptic matrix components with aggregates, in contrast, was less precise. Both laminin β2 and α5 chains, which are concentrated at synaptic sites in vivo (Patton, 2000), were concentrated at aggregates (Fig. 3, C
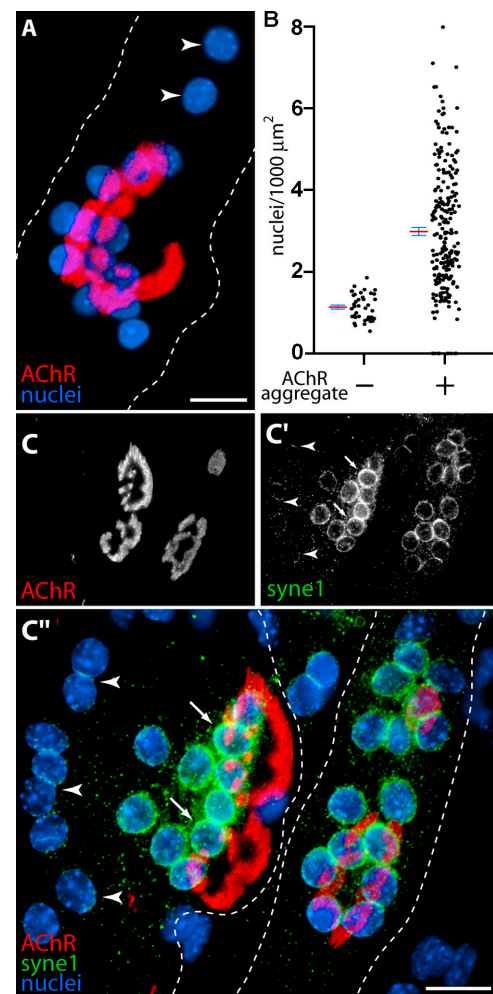

Figure 4.   **Molecularly specialized nuclei cluster at AChR aggregates in aneural myotubes cultured on laminin.** (A) DAPI-stained myonuclei (blue) cluster in apposition to branched aggregates (red); fewer nuclei are present elsewhere in the myotube (arrowheads). Dashed lines indicate myotube borders. (B) Nuclear density was quantified beneath an elliptical region defined by the extent of the AChR aggregate and in regions lacking AChR aggregates. The means of these distributions (± SEM) shows that average nuclear density is nearly threefold higher in association with aggregates ($n = 230$) than in AChR poor regions ($n = 40$). (C) Syne-1 (green) is more abundant in aggregate-associated nuclei (arrows) than in nuclei displaced from AChR aggregates (arrowheads). AChRs are red and nuclei blue, as in A. Dashed lines indicate the myotube borders. Bars: (A and C'') 20 μm.

and D). These chains were most abundant in apposition to receptor-rich branches, but staining was also present in central, AChR-poor regions of the aggregate. At adult NMJs, β2 and α5 laminin distributions mirror AChR branching patterns (Patton, 2000). One possible explanation for this dissimilarity is that matrix is deposited as aggregates grow and that mechanisms necessary for remodeling it may be present in vivo but not in vitro.

Association of AChR aggregates with specialized nuclei

As NMJs mature in vivo, myonuclei cluster beneath the postsynaptic apparatus. Staining with a nuclear dye revealed clusters of nuclei associated with AChR aggregates in vitro (Fig. 4 A). On average, nuclear density was approximately
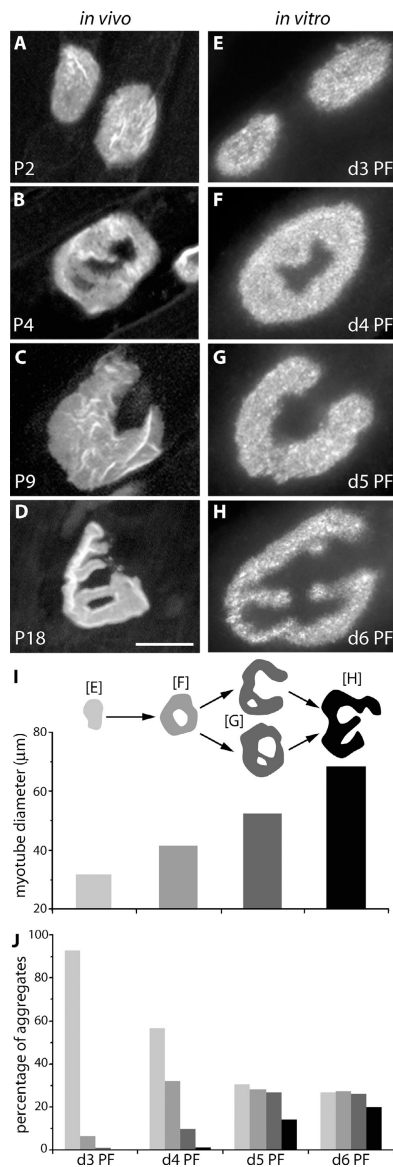
Figure 5. **Transitional AChR aggregate morphologies in vivo and in vitro.** (A–D) AChR-rich postsynaptic specializations at the NMJ are initially plaque-shaped (A), perforated (B), C-shaped (C), and branched (D) structures become successively more prevalent as development proceeds. Postnatal ages (P) are indicated in each panel. (E–H) AChR aggregates formed on laminin-coated substrates in the absence of innervation also display plaque-shaped, perforated, C-shaped, and branched shapes. PF, days after initiating fusion. (I) The diameter of myotubes bearing aggregates of the four morphological types shown in A–H. $n = 32–147$ clusters per point, from a 5-d postfusion culture. Diameter was measured at the cluster. The schematic applies to I and J. (J) The prevalence of morphologies in vitro as a function of days PF. $n = 205–232$ clusters per time point. Bar, 20 μm for all panels.

threefold higher beneath aggregates than elsewhere in the same cells (Fig. 4 B). This result shows that axons are dispensable for local accumulation of myonuclei.

Synapse-associated nuclei in myofibers are transcriptionally distinct from extrasynaptic nuclei in the same cell (Schaeffer et al., 2001). To ask whether nuclei associated with the AChR aggregates become specialized, we used antibodies to a nuclear envelope component, syne-1, which is

the only protein known to be selectively associated with synaptic nuclei (Apel et al., 2000). Nuclei associated with AChR clusters were richer in syne-1 than nonreceptor-associated nuclei in the same cell (Fig. 4 C). We also found, using in situ hybridization, that AChR α–subunit mRNA was concentrated in the vicinity of the nuclear clusters associated with AChR aggregates (unpublished data). However, the method was insufficiently quantitative to determine whether the abundance of RNA per nucleus was higher near to than far from AChR aggregates.

Differences between aneural aggregates and NMJs

Some components of the mature postsynaptic apparatus were not detected at aneural aggregates. We used fluorescently coupled fasiculin-2 to probe for the presence of acetylcholinesterase, a muscle-derived enzyme localized to the NMJ, but found none at aneural aggregates (unpublished data). Its absence may reflect the fact that acetylcholinesterase accumulation is activity dependent (Rubin et al., 1980). In addition, laminin γ_1, which is present throughout the muscle fiber basal lamina in vivo, was concentrated at aneural aggregates, and laminin α_4, which is concentrated at the mature NMJ, was not detected in vitro (Fig. 3 E and not depicted). There were also two topological features of the mature NMJ that were not evident in the aggregates: the shallow gutters in which AChR-rich branches lie and the deep folds that indent the postsynaptic membrane. The presence of folds has been documented at AChR-rich plaques in aneural myotubes (Sanes et al., 1984) and we cannot exclude the possibility that some are present at branched aggregates, but confocal and interference reflection microscopy failed to detect the striations indicative of multiple, aligned folds (unpublished data; see Marques et al., 2000 for evidence that folds can be visualized by light microscopy). Finally, there is only a single NMJ per adult muscle fiber, but some cultured myotubes bore multiple branched aggregates.

Time-lapse imaging of topological transformations

AChR aggregates at neonatal NMJs are plaque shaped. Later, ring-shaped, C-shaped, and branched forms become successively more prevalent (Slater, 1982a; Marques et al., 2000; Lanuza et al., 2002; Fig. 5, A–D). A similar array of forms was present in vitro (Fig. 5, E–H). More complex forms were preferentially associated with larger myotubes (Fig. 5 I), suggesting that they appeared sequentially as myotubes matured. To test this idea, we assessed the prevalence of simple and complex aggregates in cultures 3–6 d after inducing fusion. Aggregates resembling more mature NMJs became more common over time while clusters with simpler morphology became less prevalent (Fig. 5 J). The pace of maturation was much faster, however, in vitro than in vivo, perhaps reflecting the more rapid growth of myotubes in vitro than in vivo.

To seek direct evidence for the developmental sequence sketched in Fig. 5 I and to determine how the AChR-rich domains develop, we used time-lapse imaging. In the examples shown in Fig. 6, cultures were maintained for 5 d after myotube fusion, then stained with fluorescent Btx, and imaged three times at 12-h intervals. The cultures were restained with Btx before the final view to label all AChRs
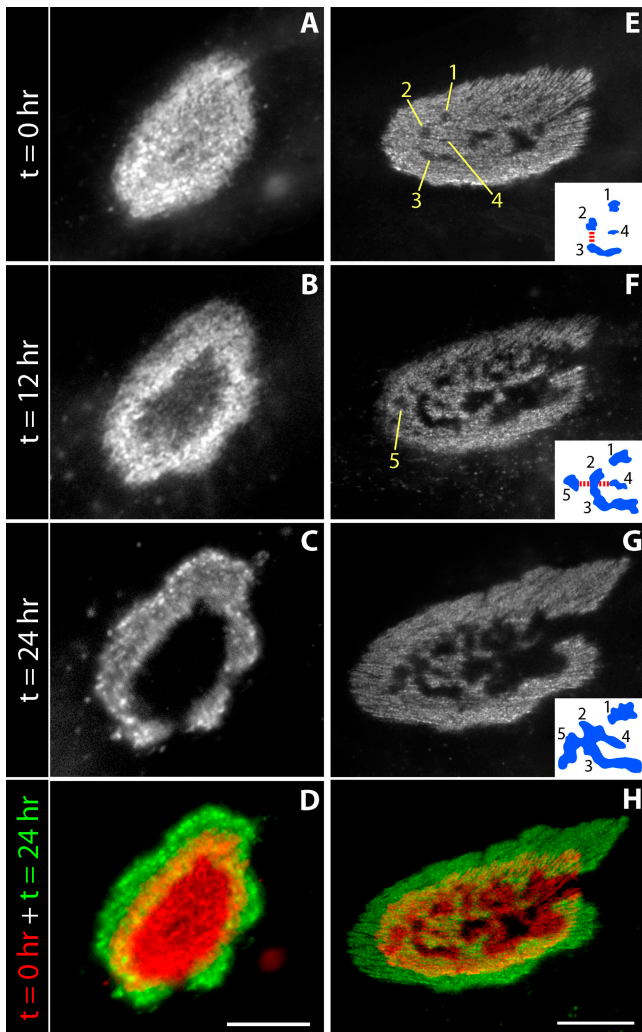
Figure 6. **Time-lapse imaging of AChR aggregates on aneural myotubes.** (A–C) Cultures were stained with Btx and imaged immediately, then after two successive 12-h intervals. Before the last time point, cultures were restained with Btx. This AChR plaque acquired a central AChR-poor hole (B) that broke through the annulus to form an "open" configuration (C). (D) Overlay of the first (red) and final images (green) shows growth of the AChR aggregate and disproportionate enlargement of the central hole. (E–G) This initially perforated aggregate developed branches by partial fusion of AChR-poor holes along part of their perimeter. Numbered perforations are sketched in the insets to show how branches form through partial fusion (red lines). (H) Overlay of the first and last time points as in D. Bars: (A–D) 10 μm; (E–H) 20 μm.

that had been added in the interim. In other experiments, cultures were imaged four times at 3-h intervals (unpublished data).

In the sequence shown in Fig. 6 (A–C), a nearly uniform plaque became perforated over a period of 12 h, and then started to become C-shaped during the next 12 h. In the sequence shown in Fig. 6 (E–G), multiple perforations in a plaque fused to form branches. These results demonstrate that plaques become pretzels by way of transitional forms resembling those observed in young muscles in vivo. Moreover, analysis of these and similar sequences ($n = 27$) revealed a series of steps by which successive forms were generated: (a) plaque-shaped aggregates increase in diameter without a ma-

jor change in their oval shape (unpublished data); (b) small AChR-poor "holes" appear near the center of the plaque (Fig. 6, A and B); (c) the holes grow disproportionately by comparison to the outer perimeter of the aggregate (Fig. 6, E–G, hole 1; see Fig. 7 H); (d) one or a few holes break through the perimeter of the aggregate forming the open side (Fig. 6, B and C); (e) other holes fuse with each other as they grow (Fig. 6, F and G, holes 4 and 5); and (f) some fusions of elongated perforations occur at their ends leaving the remaining receptors as a peninsula or branch (Fig. 6, E and F, hole 3). Together, these six processes account for much of the complexity of the pretzel-shaped aggregate.

Patterns of AChR addition to growing aggregates

The transitions documented in Figs. 5 and 6 must result from some combination of movements, additions, and losses of AChRs. To assess the patterns in which these occur, we performed two additional experiments. In the first, we asked where AChRs were added as the aggregates grew. We saturated surface AChRs with Alexa 594–coupled Btx, washed away unbound label, and incubated the cells for 12 h. After this period, cells were incubated with Alexa 488–Btx to label receptors inserted into the membrane during the preceding 12 h. After an additional 12 h, we stained with a third spectrally distinct conjugate, Alexa 647–Btx.

This experiment revealed three features of AChR addition (Fig. 7, A–D). First, each population had a distinct distribution, indicating that once AChRs were added to the cluster, they mixed with other AChR populations to only a limited extent. Second, the separate populations were systematically arranged in order of age, with younger receptors preferentially (although not exclusively) concentrated at the periphery of aggregates. Third, in aggregates that were C-shaped or branched, new AChRs were most abundant at the outer or convex margin. These results suggest complex patterning of the machinery responsible for AChR addition, loss, or mobility.
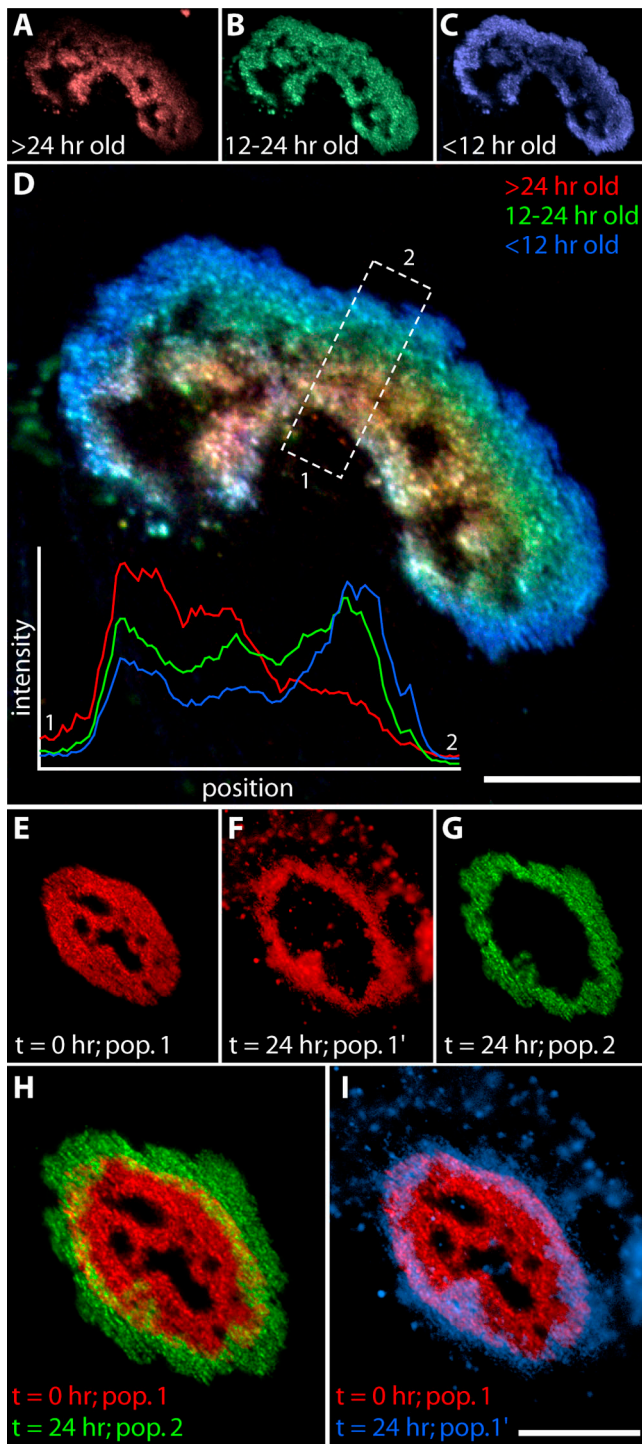
In a second set of experiments, we imaged surface AChRs immediately after labeling them, waited 24 h, labeled new AChRs with a second color, and imaged the two populations separately (Fig. 7, E–I). As above, the aggregate grew symmetrically and its AChR-poor perforation grew disproportionately (Fig. 7 H compare with Fig. 6, D and H). Despite this growth, however, the area occupied by receptors already present at t = 0 changed little (Fig. 7 I). This result provides direct evidence for the relative immobility of AChRs after membrane insertion.

We also observed that many of the AChRs present on the surface at t = 0 were subsequently found in intracellular particles, likely to be endocytic vesicles (Fig. 7, F and I; Fig. 6, B, C, and F; see Akaaboune et al., 1999 for discussion of similar observations in vivo). These vesicles were more abundant in areas near aggregates than in aggregate-free areas, suggesting that they were derived from the aggregate itself. This result raises the possibility that holes form at least in part by coupled processes of endocytic removal of AChR-rich membrane and its replacement with AChR-poor membrane.
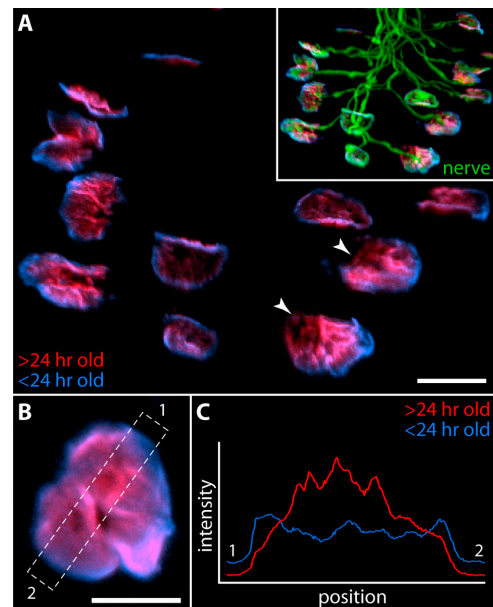
Patterns of AChR addition in vivo

To learn whether patterns of receptor addition observed in vitro resemble those at normally developing NMJs, we de-

Figure 8. **Circumferential growth of AChR clusters at the NMJ.** (A) Btx was injected above the sternomastoid muscle of a postnatal day five pup that expressed YFP in its motor axons. After 1 d, the pup was killed, and unlabeled AChRs were stained with a second, spectrally distinct Btx conjugate. AChRs carrying the first tag (red) are found preferentially near the center of aggregates, whereas younger AChRs (blue) are concentrated at the periphery. Note that in "open" aggregates (arrowheads) new AChRs are preferentially concentrated along the convex margin. The nerve invariably enters the synapse from the opposite side (inset, overlay with YFP to show pattern of innervation). (B) High resolution image of a single junction labeled as above. (C) Relative intensities of the two labels in the region boxed in B. Bars: (A) 20 µm; (B) 10 µm.

vised the following experiment: mouse pups expressing YFP in all motor axons (Feng et al., 2000) were injected above the sternomastoid muscle with Alexa 647–Btx at postnatal day five. After injection, pups were returned to their mothers for 1 d, after which the sternomastoid muscle was removed and labeled with Alexa 594–Btx. This protocol revealed a pattern similar to that observed in vitro: AChRs carrying the second tag were concentrated around the periphery of the receptor cluster (Fig. 8). In addition, in aggregates that were open at one side, new AChRs were preferentially added at the outer or convex margin, just as observed in vitro (Fig. 8 A, arrowheads compare with Fig. 7 D). There was more labeling of central areas by the final color in vivo than in vitro (Fig. 7, A–D, compare with Fig. 8) but this reflects, at least in part, differences in protocol: AChRs were not saturated by the first color in vivo (to avoid lethality from systemic Btx), nor were the first and final colors separated by an intermediate label. Thus, as seen in vitro, AChRs have limited mobility and are added in an annular, asymmetric fashion to growing end plates.

Figure 7. **Patterns of AChR addition to aneural aggregates.** (A–D) Circumferential addition of AChRs. Myotubes cultured on a laminin-coated substrate were stained with Alexa 594–Btx at 5 d after fusion (A, red), incubated 12 h, restained with Alexa 488–Btx (B, green), incubated an additional 12 h, and then stained with Alexa 647–Btx (C, blue) and imaged. Thus, each color marks AChRs that have spent a different amount of time in the membrane. Overlay (D), emphasizes the distinct distribution of each population: the oldest receptors (red) are most central, whereas the youngest (blue) are most peripheral. Inset in D shows relative intensities of the three labels in the boxed region. (E–I) Limited AChR mobility within aggregates. Cultures were stained with Alexa 594–Btx and imaged immediately (E, pop. 1). After 24 h, the cultures were stained with Alexa 488–Btx and both the original population (F, pop. 1') and the new population (G, pop. 2)

of AChRs were imaged. Overlay of population 1 (t = 0) and population 2 (t = 24 h) illustrates the growth of the AChR aggregate (H). Despite this growth, the lateral extent of the original population changed little (I; pop. 1' is pseudocolored blue). Numerous AChR-rich vesicles near the aggregate (F and I) may indicate endocytotic removal of AChRs. Bars: (D and I) 20 µm.

Discussion

Nerve-independent patterning of the postsynaptic apparatus

We found that myotubes formed and maintained in the absence of neurons construct elaborately branched aggregates of AChRs whose shape is strikingly similar to that of the adult NMJ. Moreover, AChRs in the aggregates colocalize with extracellular, transmembrane, intracellular, and nuclear markers of the postsynaptic apparatus and develop through a series of transitional forms similar to those observed during NMJ maturation. These results prove that aneural myotubes can pattern an apparatus that bears remarkable similarity to the postsynaptic site.

Why were complex aggregates not described previously? Numerous groups (including our own) have analyzed clustering of AChRs in cultured myotubes. However, in most cases myotubes were cultured on uncoated, gelatin-coated, or polycation-coated substrata, which do not promote pretzel formation. In some studies, C2 cells (Kostrominova and Tanzer, 1995; Yao et al., 1996; Adams et al., 1999), other myogenic lines (Ocalan et al., 1988), or primary myoblasts (Foster et al., 1987) were grown on laminin-coated substrates. However, in these cases postsynaptic differentiation was not assessed.

How does the substrate promote the formation of an AChR-rich domain? One possibility is that tight adhesion is critical. First, complex aggregates form exclusively at the substrate interface, and when the interface is larger, aggregates are more complex. Second, when myotubes are mechanically detached from the substrate, they leave behind postsynaptic "ghosts" enriched in AChRs, indicating a direct, tight interaction with the substrate. Third, the effect is not laminin specific: aggregates also form on fibronectin. Because fibronectin engages a largely nonoverlapping set of cell surface receptors ($\alpha_4\beta_1$ and $\alpha_5\beta_1$ integrins versus the major laminin receptors $\alpha_7\beta_1$ integrin and dystroglycan; Plow et al., 2000), the effect is likely not dependent on any specific receptor, although it might require integrin signaling generally. Finally, the AChR clustering effects of bath-applied laminin, which are receptor mediated, do not require MuSK (Sugiyama et al., 1997; Burkin et al., 1998; Marangi et al., 2002), whereas pretzel formation is MuSK dependent. Together, these data suggest that substrate-bound laminin does not act through established laminin-dependent AChR clustering pathways or a unique matrix receptor, but rather supplies a sufficiently adhesive substrate to trigger muscle-intrinsic machinery.

How might adhesion initiate postsynaptic differentiation? One possibility is that the primary effect of the adhesive substrate is to cluster and thereby activate MuSK. Multimerization activates many receptor tyrosine kinases, and for MuSK in particular, clustering with antibodies (Xie et al., 1997) or by coexpression with rapsyn (Gillespie et al., 1996) promotes agrin-independent activation. Alternatively, the interaction may be autocrine; laminin may provide a scaffold upon which the myotube deposits components normally concentrated in the synaptic cleft (Fig. 3), some of which might activate MuSK. Indeed, although it was originally thought that agrin alone activates MuSK, agrin-independent but MuSK-dependent postsynaptic differentiation has now been documented in vivo (Lin et al., 2001; Sander et al., 2001; Yang et al., 2001).

Mechanisms of postsynaptic maturation

A key question raised by this study is how a uniform coat of laminin leads to formation of an elaborately patterned array. Why does the branched array resemble a pretzel rather than, for example, a snowflake? Because the sequence of steps by which patterns form in aneural myotubes is similar to that observed in vivo (Figs. 5–8), similar mechanisms may be involved, in which case analysis in the accessible culture system might help us to understand synaptic maturation. Our observations have revealed a set of cellular phenomena that can guide future studies of molecular mechanisms that regulate this maturation.

First, branches form from plaques in a multistep process that involves the appearance of AChR-poor perforations, their asymmetric expansion, and fusion at discrete sites along shared borders. Although individually simple and few in number, combination and iteration of these steps provides a way to understand how the highly complex topology of the adult NMJ is generated. Moreover, small differences among aggregates in the number, spacing, growth, and fusion pattern of perforations can explain the great topological variation among NMJs.

Second, the formation of AChR-poor perforations within a plaque implies the existence of a mechanism for local disappearance of AChRs without a large-scale change in the AChR density nearby. Local endocytosis is a candidate mechanism for this local removal. Endocytosis has been shown to participate in the turnover of unclustered AChRs and the dispersal of AChR plaques on cultured myotubes (Pumplin and Bloch, 1987; St. John and Gordon, 2001). Our observation that AChR-containing intracellular vesicles are conspicuous as plaques perforate is consistent with the possibility that locally controlled endocytosis may act to sculpt aggregates. Current studies are aimed at documenting the topology of endocytosis during aggregate remodeling.

Third, the AChR dynamics we observed provide a way to understand how AChR-poor perforations elaborate: new AChRs are added to aggregates circumferentially, and there is limited mixing of receptor populations added at different times. As a consequence of the limited intermixing, areas that become AChR poor remain AChR poor. As a consequence of peripheral addition, lost AChRs are replaced in a manner that leads to overall aggregate growth while preserving the central AChR-poor perforations. AChRs exhibit at least some similar behaviors in vivo: Akaaboune et al. (2002) showed that mobility of AChRs at adult NMJs is limited; we were able to show constrained mobility and circumferential addition of AChRs at developing NMJs (Fig. 8); and a study by Weinberg et al. (1981) argued for a similar pattern during growth of synapses in reinnervated adult muscle based on autoradiographic techniques.

What is the source of the patterning information? An attractive possibility is that patterns result from a self-assembly process in which cytoskeletal rearrangements drive membrane remodeling. One possible parallel is the podosome belt, a geometrically complex adhesive structure formed in

another large, multinucleated cell, the osteoclast (Marchisio et al., 1984). Recent studies of these structures have provided evidence that their growth and maturation involves actin polymerization and depolymerization organized by integrins; ring formation; centrifugal expansion driven by asymmetric addition of new podosome subunits; and microtubule-based stabilization at the cell periphery (Destaing et al., 2003; Evans et al., 2003; for review see Linder and Aepfelbacher, 2003). Similarly, actin-driven movements and actin-organizing molecules (e.g., rho GTPases) have been implicated in AChR clustering (Bloch and Pumplin, 1988; Dai et al., 2000; Weston et al., 2003), although their roles in generating complex topology have not heretofore been considered. Unfortunately, although actin (stained with phalloidin) is concentrated in regions of complex AChR aggregates, attempts to demonstrate that other components of focal adhesion plaques, podosomes, or endocytic compartments (e.g., paxillin, integrin subunits, or rab5a) colocalize with the aggregates have so far been unsuccessful (unpublished data). Therefore, we do not yet have satisfying insights into the machinery that assembles these structures.

The patterns of receptor addition we observed may be common to several types of junctions. A recent study of gap junctions demonstrated that they grow by addition of subunits (connexins) in an "inside-out" pattern parallel to that documented here for AChRs (Gaietta et al., 2002). Similar processes may occur at neuron–neuron synapses, but their small size has so far made it impossible to learn where receptors are added or removed as these synapses grow and remodel (Passafaro et al., 2001; Rosenberg et al., 2001). In contrast, the large size and accessibility of the aggregates we describe allow these issues to be addressed.

A postsynaptic influence on presynaptic topology?

The observation that aneural myotubes form AChR aggregates with similar morphology to those at NMJs raises the possibility that postsynaptic topology may influence presynaptic branch patterns rather than (or in addition to) the other way around. The obvious difficulty with this view is that it appears inconsistent with the sequence of events that occurs during normal development, in which the axon forms a rudimentary terminal arbor before the postsynaptic apparatus becomes branched (Sanes and Lichtman, 1999). In fact, however, many previous observations are consistent with a postsynaptic influence on presynaptic morphology. First, during normal development, some AChR-rich plaques form on portions of the myotube surface that axons have not yet contacted (Dahm and Landmesser, 1991), and even when embryonic muscles are rendered aneural in vivo, AChR plaques form in the central region that axons would have contacted (Lin et al., 2001; Yang et al., 2001; Arber et al., 2002). Thus, growing axons may sometimes contact preformed AChR clusters, rather than inducing new ones. Second, early topological transitions, including the appearance of receptor-poor perforations in the plaque, often precede local axonal remodeling (Balice-Gordon and Lichtman, 1993). This sequence has led to the hypothesis that loss of postsynaptic specializations from a restricted region leads to withdrawal of an axonal branch from that region. Third, likewise, regions of developing NMJs that are vacated by retracting axons are often reoccupied by other axon branches, a process dubbed "synaptic takeover" (Walsh and Lichtman, 2003). Fourth, when motor axons contact MuSK$^{-/-}$ or rapsyn$^{-/-}$ myotubes, in which postsynaptic differentiation is blocked, they fail to form arbors (Nguyen et al., 2000). Fifth, although neonatal denervation largely arrests postsynaptic maturation, some AChR-poor holes do appear and grow even after denervation (Slater, 1982b; unpublished data). Sixth, growth of muscle fibers during late stages of maturation or in response to androgens results in symmetrical enlargement of the postsynaptic apparatus, which is matched by presynaptic growth, maintaining precise alignment of pre- and postsynaptic structures (Balice-Gordon et al., 1990). Finally, during reinnervation, the pattern of nerve terminal branches is determined by postsynaptic morphology (Sanes et al., 1978; Rich and Lichtman, 1989). Thus, there is reason to believe that muscle-intrinsic patterning of the postsynaptic array could determine the pattern of axon terminal branches during development.

Finally, we emphasize that the ability of the myotube to generate an NMJ-like pattern does not preclude a critical role for the nerve. Postsynaptic structures may not only exert retrograde influences on nerve terminal branches but also receive anterograde influences from the nerve. A precedent is provided by studies in which focal inactivation of AChRs in small regions of adult junctions, interpreted as mimicking focal loss of neurotransmission, resulted in focal loss of AChRs, followed by withdrawal of overlying axonal branches (Balice-Gordon and Lichtman, 1994). During development, for example, areas of decreased synaptic efficacy could lead to local loss of AChRs and associated matrix molecules, which would act back to cause withdrawal of presynaptic branches. Similarly, the open side of the AChR cluster might form randomly in isolation, but locally restricted activity due to myelination of the preterminal axon may bias the polarization of the cluster in vivo. This could account for the observation that the nerve nearly always enters the NMJ from the open side (Marques et al., 2000).

Materials and methods

Tissue culture

The C2C12 subclone of the C2 myogenic cell line was obtained from American Type Culture Collection and carried on gelatin-coated dishes in DME supplemented with penicillin, streptomycin, and 20% FCS. Myogenic lines generated from MuSK$^{-/-}$ (Sugiyama et al., 1997), rapsyn$^{+/+}$, and rapsyn$^{-/-}$ muscles (Fuhrer et al., 1999) were obtained from D. Glass (Regeneron Pharmaceuticals) and C. Fuhrer (University of Zurich, Zurich, Switzerland), respectively. MuSK$^{-/-}$ cells were carried as described previously by Zhou et al. (1999). Rapsyn$^{+/+}$ and rapsyn$^{-/-}$ myoblasts were carried on Matrigel-coated (Becton Dickinson) dishes in C2C12 media supplemented with 20 U/ml γ-interferon (R&D Systems) and 2% chick embryo extract at 33°C, then transferred to laminin-coated dishes for fusion and analysis. Primary myotubes were cultured as described previously by Gautam et al. (1995, 1996). In some cases, 10 μM TTX (Sankyo) was added to primary cultures with the differentiation medium to inhibit contraction.

Cells were trypsinized and replated onto 8-well Permanox chamber slides (Nalge International) for histological studies or onto 60-mm Permanox dishes for time-lapse imaging. Before plating, dishes were coated with 5 μg/ml polyornithine (Sigma-Aldrich) in distilled water for 30 min and air dried. For laminin or fibronectin coating, a 10 μg/ml solution of EHS laminin (Invitrogen) or a 20 μg/ml solution of human fibronectin (Sigma-Aldrich) in L-15 medium supplemented with 0.2% NaHCO₃ was incubated over polyornithine-coated dishes overnight at 37°C, and aspirated immediately before plating cells. Myoblasts were grown to conflu-

ency and switched to DME plus 2% horse serum with penicillin and strep-tomycin to induce fusion. Cells were incubated at 37°C, 5% CO_2 for 3–7 d after fusion. For MuSK rescue experiments, $MuSK^{-/-}$ myoblasts were trans-fected with either GFP-MuSK or GFP alone using FuGENE 6 transfection reagent (Roche) at the time of plating (Zhou et al., 1999).

Analysis of cultured myotubes

Live myotubes were incubated with 1 μg/ml of fluorescently coupled Btx (Molecular Probes) for 30 min to label AChRs. The cells were washed with PBS, fixed in 4% PFA in PBS, and washed again in PBS before mounting in glycerol plus 1 mg/ml paraphenylenediamine for immediate visualization or scavenged with 50 mM lysine in PBS plus 0.1% (vol/vol) Triton X-100 for immunostaining. Nonspecific staining was blocked with a solution of 2% BSA and 2% goat serum in PBS plus 0.1% Triton X-100 before overnight in-cubation with rabbit anti-GFP (CHEMICON International, Inc.), rabbit anti-rapsyn (Gautam et al., 1995), mouse antiphosphotyrosine (clone PY20; BD Transduction Labs), rabbit anti–β_2 laminin (a gift from R. Timpl, Max Planck Institut of Biochemistry, Martinsried, Germany), rabbit anti–α_5 laminin (Miner et al., 1997), rat anti–γ_1 laminin (clone 1914; CHEMICON Interna-tional, Inc.), or rabbit anti–syne-1 (Apel et al., 2000). In the case of γ_1 stain-ing, cells were cultured on a substrate of 10 μg/ml of rat laminin-1 (Telios Pharmaceuticals,) with which the antibody does not cross react. Primary antibodies were detected with Cy3- or Alexa 488–coupled goat secondary antibodies (Molecular Probes). In some cases cells were incubated with DAPI (Molecular Probes) for 5 min to visualize nuclei.

To distinguish newly inserted AChRs from older receptors in culture, we stained myotubes with Alexa 594–Btx for 30 min, washed the cells with differentiation media, and returned them to the incubator for 12–24 h. Newly inserted AChRs were then stained with Alexa 488–Btx and the cells were collected. For some experiments we used Alexa 647–Btx as a third label after an additional 12 h of incubation.

Epifluorescence images of fixed cells were collected on an Axioplan2 microscope (Carl Zeiss MicroImaging, Inc.) fitted with a MagnaFire CCD camera (Optronics). Multiple time point observations of individual AChR aggregates labeled with Btx were collected on a microscope (model BX50; Olympus) equipped with a cooled CCD camera (model MicroMax; Prince-ton Instruments Inc.) and a 100X dipping cone water immersion lens (NA 1.0). To reduce phototoxicity, the myotubes were kept in phenol red-free medium buffered with Hepes for the duration of the imaging sessions. Be-tween time points the cells were returned to the incubator in their differen-tiation medium.

Confocal images were obtained on a confocal laser scanning micro-scope (model FV500; Olympus) equipped with Krypton/Argon/HeNe la-sers using a 60X oil objective (NA 1.4). Images were analyzed with Metamorph software (Universal Imaging Corp.) and edited with Adobe Photoshop version 6. All confocal images are z stacks flattened in Meta-morph. Nuclear density in postsynaptic regions was determined by count-ing nuclei enclosed within an elliptical border fitted to each AChR cluster. Extrasynaptic nuclear density was measured similarly for regions lacking AChR clusters.

Analysis of the NMJ

Muscles were dissected from transgenic mice in which all motor axons are marked with YFP (line YFP-16; Feng et al., 2000). Muscles were fixed over-night in 4% PFA, washed, and stained with 1 μg/ml Alexa 594–Btx over-night to label AChRs. To distinguish newly inserted AChRs from older recep-tors in vivo, postnatal day five YFP-16 mouse pups were injected near the sternomastoid muscle with 100 μl of a 1 μg/ml solution of Alexa 647–Btx in sterile saline. Pups were returned to their mothers for 1 d before they were killed and the sternomastoid fixed and stained with Alexa 594–Btx. Images were obtained as described previously (Analysis of cultured myotubes).

References

Adams, J.C., J.D. Clelland, G.D. Collett, F. Matsumura, S. Yamashiro, and L. Zhang. 1999. Cell-matrix adhesions differentially regulate fascin phosphory-lation. *Mol. Biol. Cell.* 10:4177–4190.

Akaaboune, M., S.M. Culican, S.G. Turney, and J.W. Lichtman. 1999. Rapid and reversible effects of activity on acetylcholine receptor density at the neuro-muscular junction in vivo. *Science.* 286:503–507.

Akaaboune, M., R.M. Grady, S. Turney, J.R. Sanes, and J.W. Lichtman. 2002. Neurotransmitter receptor dynamics studied in vivo by reversible photo-unbinding of fluorescent ligands. *Neuron.* 34:865–876.

Anderson, M.J., and M.W. Cohen. 1977. Nerve-induced and spontaneous redistri-bution of acetylcholine receptors on cultured muscle cells. *J. Physiol.* 268: 757–773.

Apel, E.D., R.M. Lewis, R.M. Grady, and J.R. Sanes. 2000. Syne-1, a dystrophin- and Klarsicht-related protein associated with synaptic nuclei at the neuro-muscular junction. *J. Biol. Chem.* 275:31986–31995.

Arber, S., S.J. Burden, and A.J. Harris. 2002. Patterning of skeletal muscle. *Curr. Opin. Neurobiol.* 12:100–103.

Balice-Gordon, R.J., S.M. Breedlove, S. Bernstein, and J.W. Lichtman. 1990. Neuromuscular junctions shrink and expand as muscle fiber size is manipu-lated: in vivo observations in the androgen-sensitive bulbocavernosus muscle of mice. *J. Neurosci.* 10:2660–2671.

Balice-Gordon, R.J., and J.W. Lichtman. 1993. In vivo observations of pre- and postsynaptic changes during the transition from multiple to single innerva-tion at developing neuromuscular junctions. *J. Neurosci.* 13:834–855.

Balice-Gordon, R.J., and J.W. Lichtman. 1994. Long-term synapse loss induced by focal blockade of postsynaptic receptors. *Nature.* 372:519–524.

Bloch, R.J. 1979. Dispersal and reformation of acetylcholine receptor clusters of cultured rat myotubes treated with inhibitors of energy metabolism. *J. Cell Biol.* 82:626–643.

Bloch, R.J., and D.W. Pumplin. 1988. Molecular events in synaptogenesis: nerve-muscle adhesion and postsynaptic differentiation. *Am. J. Physiol.* 254:C345–C364.

Burgess, R.W., Q.T. Nguyen, Y.J. Son, J.W. Lichtman, and J.R. Sanes. 1999. Al-ternatively spliced isoforms of nerve- and muscle-derived agrin: their roles at the neuromuscular junction. *Neuron.* 23:33–44.

Burkin, D.J., M. Gu, B.L. Hodges, J.T. Campanelli, and S.J. Kaufman. 1998. A functional role for specific spliced variants of the α7β1 integrin in acetylcho-line receptor clustering. *J. Cell Biol.* 143:1067–1075.

Dahm, L.M., and L.T. Landmesser. 1991. The regulation of synaptogenesis during normal development and following activity blockade. *J. Neurosci.* 11:238–255.

Dai, Z., X. Luo, H. Xie, and H.B. Peng. 2000. The actin-driven movement and formation of acetylcholine receptor clusters. *J. Cell Biol.* 150:1321–1334.

DeChiara, T.M., D.C. Bowen, D.M. Valenzuela, M.V. Simmons, W.T. Pou-eymirou, S. Thomas, E. Kinetz, D.L. Compton, E. Rojas, J.S. Park, et al. 1996. The receptor tyrosine kinase MuSK is required for neuromuscular junction formation in vivo. *Cell.* 85:501–512.

Destaing, O., F. Saltel, J.C. Geminard, P. Jurdic, and F. Bard. 2003. Podosomes display actin turnover and dynamic self-organization in osteoclasts express-ing actin-green fluorescent protein. *Mol. Biol. Cell.* 14:407–416.

Evans, J.G., I. Correia, O. Krasavina, N. Watson, and P. Matsudaira. 2003. Mac-rophage podosomes assemble at the leading lamella by growth and fragmen-tation. *J. Cell Biol.* 161:697–705.

Feng, G., R.H. Mellor, M. Bernstein, C. Keller-Peck, Q.T. Nguyen, M. Wallace, J.M. Nerbonne, J.W. Lichtman, and J.R. Sanes. 2000. Imaging neuronal subsets in transgenic mice expressing multiple spectral variants of GFP. *Neu-ron.* 28:41–51.

Ferns, M., W. Hoch, J.T. Campanelli, F. Rupp, Z.W. Hall, and R.H. Scheller. 1992. RNA splicing regulates agrin-mediated acetylcholine receptor cluster-ing activity on cultured myotubes. *Neuron.* 8:1079–1086.

Fischbach, G.D., and S.A. Cohen. 1973. The distribution of acetylcholine sensitiv-ity over uninnervated and innervated muscle fibers grown in cell culture. *Dev. Biol.* 31:147–162.

Foster, R.F., J.M. Thompson, and S.J. Kaufman. 1987. A laminin substrate pro-motes myogenesis in rat skeletal muscle cultures: analysis of replication and development using antidesmin and anti-BrdUrd monoclonal antibodies. *Dev. Biol.* 122:11–20.

Frank, E., and G.D. Fischbach. 1979. Early events in neuromuscular junction for-mation in vitro: induction of acetylcholine receptor clusters in the postsyn-aptic membrane and morphology of newly formed synapses. *J. Cell Biol.* 83: 143–158.

Fuhrer, C., M. Gautam, J.E. Sugiyama, and Z.W. Hall. 1999. Roles of rapsyn and agrin in interaction of postsynaptic proteins with acetylcholine receptors. *J. Neurosci.* 19:6405–6416.

Gaietta, G., T.J. Deerinck, S.R. Adams, J. Bouwer, O. Tour, D.W. Laird, G.E. Sosinsky, R.Y. Tsien, and M.H. Ellisman. 2002. Multicolor and electron

microscopic imaging of connexin trafficking. *Science.* 296:503–507.

Gautam, M., P.G. Noakes, J. Mudd, M. Nichol, G.C. Chu, J.R. Sanes, and J.P. Merlie. 1995. Failure of postsynaptic specialization to develop at neuromuscular junctions of rapsyn-deficient mice. *Nature.* 377:232–236.

Gautam, M., P.G. Noakes, L. Moscoso, F. Rupp, R.H. Scheller, J.P. Merlie, and J.R. Sanes. 1996. Defective neuromuscular synaptogenesis in agrin-deficient mutant mice. *Cell.* 85:525–535.

Gautam, M., T.M. DeChiara, D.J. Glass, G.D. Yancopoulos, and J.R. Sanes. 1999. Distinct phenotypes of mutant mice lacking agrin, MuSK, or rapsyn. *Brain Res. Dev. Brain Res.* 114:171–178.

Gesemann, M., A.J. Denzer, and M.A. Ruegg. 1995. Acetylcholine receptor-aggregating activity of agrin isoforms and mapping of the active site. *J. Cell Biol.* 128:625–636.

Gillespie, S.K., S. Balasubramanian, E.T. Fung, and R.L. Huganir. 1996. Rapsyn clusters and activates the synapse-specific receptor tyrosine kinase MuSK. *Neuron.* 16:953–962.

Kostrominova, T.Y., and M.L. Tanzer. 1995. Rodent myoblast interactions with laminin require cell surface glycoconjugates but not laminin glycosyl groups. *J. Cell. Biochem.* 57:163–172.

Lanuza, M.A., N. Garcia, M. Santafe, C.M. Gonzalez, I. Alonso, P.G. Nelson, and J. Tomas. 2002. Pre- and postsynaptic maturation of the neuromuscular junction during neonatal synapse elimination depends on protein kinase C. *J. Neurosci. Res.* 67:607–617.

Lin, W., R.W. Burgess, B. Dominguez, S.L. Pfaff, J.R. Sanes, and K.F. Lee. 2001. Distinct roles of nerve and muscle in postsynaptic differentiation of the neuromuscular synapse. *Nature.* 410:1057–1064.

Linder, S., and M. Aepfelbacher. 2003. Podosomes: adhesion hot-spots of invasive cells. *Trends Cell Biol.* 13:376–385.

Marangi, P.A., S.T. Wieland, and C. Fuhrer. 2002. Laminin-1 redistributes postsynaptic proteins and requires rapsyn, tyrosine phosphorylation, and Src and Fyn to stably cluster acetylcholine receptors. *J. Cell Biol.* 157:883–895.

Marchisio, P.C., D. Cirillo, L. Naldini, M.V. Primavera, A. Teti, and A. Zambonin-Zallone. 1984. Cell-substratum interaction of cultured avian osteoclasts is mediated by specific adhesion structures. *J. Cell Biol.* 99:1696–1705.

Marques, M.J., J.A. Conchello, and J.W. Lichtman. 2000. From plaque to pretzel: fold formation and acetylcholine receptor loss at the developing neuromuscular junction. *J. Neurosci.* 20:3663–3675.

Miner, J.H., B.L. Patton, S.I. Lentz, D.J. Gilbert, W.D. Snider, N.A. Jenkins, N.G. Copeland, and J.R. Sanes. 1997. The laminin α chains: expression, developmental transitions, and chromosomal locations of α1-5, identification of heterotrimeric laminins 8-11, and cloning of a novel α3 isoform. *J. Cell Biol.* 137:685–701.

Moss, B.L., and S.M. Schuetze. 1987. Development of rat soleus endplate membrane following denervation at birth. *J. Neurobiol.* 18:101–118.

Nguyen, Q.T., Y.J. Son, J.R. Sanes, and J.W. Lichtman. 2000. Nerve terminals form but fail to mature when postsynaptic differentiation is blocked: in vivo analysis using mammalian nerve-muscle chimeras. *J. Neurosci.* 20:6077–6086.

Ocalan, M., S.L. Goodman, U. Kuhl, S.D. Hauschka, and K. von der Mark. 1988. Laminin alters cell shape and stimulates motility and proliferation of murine skeletal myoblasts. *Dev. Biol.* 125:158–167.

Passafaro, M., V. Piech, and M. Sheng. 2001. Subunit-specific temporal and spatial patterns of AMPA receptor exocytosis in hippocampal neurons. *Nat. Neurosci.* 4:917–926.

Patton, B.L. 2000. Laminins of the neuromuscular system. *Microsc. Res. Tech.* 51:247–261.

Plow, E.F., T.A. Haas, L. Zhang, J. Loftus, and J.W. Smith. 2000. Ligand binding to integrins. *J. Biol. Chem.* 275:21785–21788.

Pumplin, D.W., and R.J. Bloch. 1987. Disruption and reformation of the acetylcholine receptor clusters of cultured rat myotubes occur in two distinct stages. *J. Cell Biol.* 104:97–108.

Qu, Z.C., E. Moritz, and R.L. Huganir. 1990. Regulation of tyrosine phosphorylation of the nicotinic acetylcholine receptor at the rat neuromuscular junc-

tion. *Neuron.* 4:367–378.

Rich, M.M., and J.W. Lichtman. 1989. In vivo visualization of pre- and postsynaptic changes during synapse elimination in reinnervated mouse muscle. *J. Neurosci.* 9:1781–1805.

Rosenberg, M., J. Meier, A. Triller, and C. Vannier. 2001. Dynamics of glycine receptor insertion in the neuronal plasma membrane. *J. Neurosci.* 21:5036–5044.

Rubin, L.L., S.M. Schuetze, C.L. Weill, and G.D. Fischbach. 1980. Regulation of acetylcholinesterase appearance at neuromuscular junctions in vitro. *Nature.* 283:264–267.

Sander, A., B.A. Hesser, and V. Witzemann. 2001. MuSK induces in vivo acetylcholine receptor clusters in a ligand-independent manner. *J. Cell Biol.* 155:1287–1296.

Sanes, J.R., and J.W. Lichtman. 1999. Development of the vertebrate neuromuscular junction. *Annu. Rev. Neurosci.* 22:389–442.

Sanes, J.R., and J.W. Lichtman. 2001. Induction, assembly, maturation and maintenance of a postsynaptic apparatus. *Nat. Rev. Neurosci.* 2:791–805.

Sanes, J.R., L.M. Marshall, and U.J. McMahan. 1978. Reinnervation of muscle fiber basal lamina after removal of myofibers. Differentiation of regenerating axons at original synaptic sites. *J. Cell Biol.* 78:176–198.

Sanes, J.R., D.H. Feldman, J.M. Cheney, and J.C. Lawrence, Jr. 1984. Brain extract induces synaptic characteristics in the basal lamina of cultured myotubes. *J. Neurosci.* 4:464–473.

Schaeffer, L., A. de Kerchove d'Exaerde, and J.P. Changeux. 2001. Targeting transcription to the neuromuscular synapse. *Neuron.* 31:15–22.

Slater, C.R. 1982a. Postnatal maturation of nerve-muscle junctions in hindlimb muscles of the mouse. *Dev. Biol.* 94:11–22.

Slater, C.R. 1982b. Neural influence on the postnatal changes in acetylcholine receptor distribution at nerve-muscle junctions in the mouse. *Dev. Biol.* 94:23–30.

St John, P.A., and H. Gordon. 2001. Agonists cause endocytosis of nicotinic acetylcholine receptors on cultured myotubes. *J. Neurobiol.* 49:212–223.

Steinbach, J.H. 1981. Developmental changes in acetylcholine receptor aggregates at rat skeletal neuromuscular junctions. *Dev. Biol.* 84:267–276.

Sugiyama, J.E., D.J. Glass, G.D. Yancopoulos, and Z.W. Hall. 1997. Laminin-induced acetylcholine receptor clustering: an alternative pathway. *J. Cell Biol.* 139:181–191.

Vogel, Z., A.J. Sytkowski, and M.W. Nirenberg. 1972. Acetylcholine receptors of muscle grown in vitro. *Proc. Natl. Acad. Sci. USA.* 69:3180–3184.

Walsh, M.K., and J.W. Lichtman. 2003. In vivo time-lapse imaging of synaptic takeover associated with naturally occurring synapse elimination. *Neuron.* 37:67–73.

Weinberg, C.B., C.G. Reiness, and Z.W. Hall. 1981. Topographical segregation of old and new acetylcholine receptors at developing ectopic endplates in adult rat muscle. *J. Cell Biol.* 88:215–218.

Weston, C., C. Gordon, G. Teressa, E. Hod, X.D. Ren, and J. Prives. 2003. Cooperative regulation by Rac and Rho of agrin-induced acetylcholine receptor clustering in muscle cells. *J. Biol. Chem.* 278:6450–6455.

Xie, M.H., J. Yuan, C. Adams, and A. Gurney. 1997. Direct demonstration of MuSK involvement in acetylcholine receptor clustering through identification of agonist ScFv. *Nat. Biotechnol.* 15:768–771.

Yaffe, D., and O. Saxel. 1977. Serial passaging and differentiation of myogenic cells isolated from dystrophic mouse muscle. *Nature.* 270:725–727.

Yang, X., S. Arber, C. William, L. Li, Y. Tanabe, T.M. Jessell, C. Birchmeier, and S.J. Burden. 2001. Patterning of muscle acetylcholine receptor gene expression in the absence of motor innervation. *Neuron.* 30:399–410.

Yao, C.C., B.L. Ziober, A.E. Sutherland, D.L. Mendrick, and R.H. Kramer. 1996. Laminins promote the locomotion of skeletal myoblasts via the alpha 7 integrin receptor. *J. Cell Sci.* 109:3139–3150.

Zhou, H., D.J. Glass, G.D. Yancopoulos, and J.R. Sanes. 1999. Distinct domains of MuSK mediate its abilities to induce and to associate with postsynaptic specializations. *J. Cell Biol.* 146:1133–1146.